Studies on Droplet-Turbulence Interactions

Y. M. Kim*, H. M. Shang and C. P. Chen****

(Received February 2, 1994)

The present study focuses on numerical modeling for droplet dispersion by turbulence and turbulence modulation by droplets. To account for the dense spray effects, modulation models, a droplet collision model, and the Reitz's wave instability breakup model are incorporated into a state-of-the-art multiphase all-speed transient flow solution procedure. A parcel probability density function(PDF) approach is implemented to improve the efficiency in droplet dispersion calculations. The numerical results indicate that the present parcel PDF model has the capability to realistically represent turbulent dispersion in dilute and dense sprays with improved efficiency over the delta function stochastic separated flow(SSF) model. Comparative performance of the existing turbulence modulation models are discussed in detail.

Key Words: Parcel PDF, Droplet Dispersion, Turbulence Modulation, Breakup, Collision

1. Introduction

Liquid fuel sprays in turbulent flows have many practical applications such as gas turbine combustors, diesel engines, rocket engines, and furnaces. Despite its important applications, our understanding of sprays is relatively limited due to complex interactions between the discrete droplet phase and the continuous gas phase. Thus, the comprehensive predicative modelling for turbulent spray combustions requires realistic representation of the interphase exchange processes in context with a mathematical formulation of multiphase dynamics.

Various approaches have been suggested to model the interphase transport phenomena. The methodologies for the spray combustion computations are largely classified as the discrete droplet model, the statistical droplet model, and the two-fluid continuum model. Comparative performances of these three approaches are well summarized in Ref.(Sirignano, 1986). Among three models, the discrete droplet model has gained wide acceptance due to its computational efficiency, the flexibility in handling poly-disperse spray, the convenient interphase coupling, and the elimination of numerical diffusion. With Eulerian-Lagrangian formulations in multi-phase flows, the stochastic separated flow(SSF) approach (Faeth, 1987) categorized in the discrete droplet model is usually employed to account for the turbulence effects on the interphase transport. In the stochastic separated flow(SSF) approach, each computational parcel represents a collection of liquid droplets having the same droplet characteristics. A random sampling technique is entailed for instantaneous gas flow properties based on a specified turbulence model and the resulting fluctuations are used in the droplet-phase Lagrangian computations for the droplet tracking. The stochastic process requires a large number of computational particles to produce satisfactory dispersion distributions even for rather dilute sprays. There are several research efforts (Litchford et al., 1991; Zhou et al., 1992; Kim et al., 1992; Shang et al., 1992) to overcome this deficiency by introducing a probability density distribution to each computational parcel representing a group of physical particles. This type of approach can be named as the parcel PDF model or the dispersion width (group) transport

* Department of Mechanical Engineering, Hanyang University, Seoul, 133-791, Korea.
** Department of Chemical Engineering, University of Alabama in Huntsville, AL35899, U.S.A.

model. This parcel PDF model can account for the turbulent droplet dispersion within each group. Each group (width) grows due to the turbulent dispersion of droplets when the computational parcel travels in the Lagrangian coordinate. The mean position of each group, determined from a deterministic or stochastic Lagrangian tracking, is taken to represent the mean of its corresponding probability density function(PDF). The variance of each PDF is represented by a statistical mean-squared dispersion which depends on prior eddy interactions. The present parcel PDF method has potential advantages to reduce the number of computational parcels with accurate representation of the spray dynamics as well as to eliminate numerically oriented noises associated with the droplet injection.

Another area of spray combustion research which is still under-explored involves the turbulence modulation due to the presence of the dispersed droplets. Specifically, modification of the properties of turbulent interphase transport rates cannot be properly represented by mean properties in the interphase transport rate expressions. It has been found (Faeth, 1987 ; Mostafa et al., 1988) that the presence of even low concentration of particulates in a turbulent mixing stream exerts a significant influence on the turbulent intensity level in the carrier fluid. In spray combustion applications, the droplet-turbulence interaction plays a very important role in the combustion process since it influences the level of mixedness of the oxidizer and the fuel vapor released from the evaporation process as well as the efficiency of the combustion process. Recently, the issue of turbulence modulation effect has been discussed extensively in Ref.(Faeth, 1987). To account for the dense spray effects, the present study employs several existing modulation models (Mostafa et al., 1988 ; Chen et al., 1985 ; Amsden et al., 1989) and the Reitz's wave instability breakup model (Reitz, 1987).

To evaluate the prediction capability of the present parcel PDF model, computations were performed for the particle dispersion in nearly-homogeneous turbulence, a particle laden round jet in inhomogeneous turbulence, and the non-evaporating solid-cone dense sprays. The numerical results indicate that the present parcel PDF model has the capability of realistically representing turbulent dispersion in dilute and dense sprays with improved efficiency over the delta function stochastic separated flow(SSF) model. In the non-evaporating solid-cone dense spray case, the predictions with the turbulence modulation model show a good agreement with available experimental data in terms of gas/drop mean and RMS velocities.

2. Mathematical Formulations

All the gas-phase and liquid-phase processes are modeled by a system of unsteady, multi-dimensional equations. The gas-phase equation is written in an Eulerian coordinate whereas the liquid-phase is presented in Lagrangian coordinates. The two-way coupling between the two phases is described by the interaction source terms. The two-equation k-ε model based on an eddy viscosity concept is used to characterize the time and length scales of the gas-phase turbulence for modelling the droplet dispersion and the turbulence modulation. These equations are given below.

2.1 Gas-phase equations

In the non-evaporating multi-phase flows, the conservation equation of mass, momentum, and turbulent transport quantities in an Eulerian coordinate can be written as follows :

$$\frac{\partial\rho}{\partial t}+\frac{\partial}{\partial x_j}(\rho U_j)=0, \tag{1}$$

$$\frac{\partial\rho U_i}{\partial t}+\frac{\partial}{\partial x_j}(\rho U_i U_j) =-\frac{\partial p}{\partial x_i}-\frac{\partial}{\partial x_j}\left(\frac{\mu_{eff}\partial U_i}{\partial x_j}\right)+S_{u_i}+S_{u_i,p}, \tag{2}$$

$$\frac{\partial\rho k}{\partial t}+\frac{\partial}{\partial x_j}(\rho U_j k) =\frac{\partial}{\partial x_j}\left(\frac{\mu_{eff}}{\sigma_k}\frac{\partial k}{\partial x_j}\right)+\rho G_k-\rho\varepsilon+S_{k,p}, \tag{3}$$

$$\frac{\partial\rho\varepsilon}{\partial t}+\frac{\partial}{\partial x_j}(\rho U_j\varepsilon) =\frac{\partial}{\partial x_j}\left(\frac{\mu_{eff}}{\sigma_\varepsilon}\frac{\partial\varepsilon}{\partial x_j}\right)+\frac{\rho\varepsilon}{k}(C_1G_k-C_2\varepsilon)+S_{\varepsilon,p}, \tag{4}$$

where ρ is the mean density of the mixture, U_i is the i^{th} component of the mean velocity, p is the mean pressure, G_k is the turbulence production term, and μ_{eff} is the effective viscosity. S_{u_i} and $S_{u_{i,p}}$ represents the gas-phase source terms and the interphase interaction source terms due to the fuel spray, respectively. Extra source terms, $S_{k,p}$ and $S_{\varepsilon,p}$, appearing Eqs. (3) and (4) represent the turbulence modulation effects by droplets. These two-phase interaction source terms will be defined later. Empirical constants in the k-ε model are taken as $\sigma_k=1.0$, $\sigma_\varepsilon=1.3$, $C_1=1.44$, $C_2=1.92$, and $C_\mu=0.09$.

2.2 SSF modeling for droplet dispersion

The spray dynamics is described by a discrete particle method formulated on a Lagrangian frame. Each computational particle represents a number of droplets having equal location, velocity, size, and temperature. The droplet-phase momentum equation can be written as:

$$\frac{dv_i}{dt}=\frac{U_i+u_i'-v_i}{\tau}+f_i. \tag{5}$$

Here, f_i represents the body force per unit particle mass, v_i and u_i' denote the particle velocity and the turbulent fluctuating gas-phase velocity, respectively. The particle relaxation time τ can be expressed as:

$$\tau^{-1}=\frac{3}{4}C_D\frac{\rho}{d_p}\,|U_i+u_i'-v_i|, \tag{6}$$

where C_D is the drag coefficient. The particle trajectory for each computational parcel can be determined by integrating the following equation.

$$\frac{dx_i}{dt}=v_i. \tag{7}$$

In the point delta function SSF model, the turbulence effects on droplet dispersion are simulated by a Monte Carlo method. With assumption of the isotropic turbulence, each component of u_i' randomly chosen from a Gaussian distribution with standard deviation $\sqrt{\frac{2}{3}k}$ is added to the mean gas velocity. This fluctuating velocity u_i' producing the particle turbulent dispersion is assumed fully correlated through an eddy life time. A new u_i' is sampled once every particle-eddy interaction time which is the minimum of the eddy life time and the particle residence time in the eddy. The detailed expressions for the interaction time, the eddy life time, and the eddy length scale can be found Ref.(Chen et al., 1992; Fasola et al., 1990; Shuen et al., 1985).

2.3 Parcel PDF method for droplet dispersion calculations

In this study, the spray is described by a discrete particle method formulated on a Lagrangian frame. To account for turbulence dispersion, we follow the dispersion width transport approach (Litchford and Jeng, 1991) which combines a normal (Gaussian) probability distribution for each computational particle. The location calculated by Eqs. (5) and (7) only represents the mean of each particle's corresponding probability function. The variance of each parcel pdf has to be calculated and the combined pdfs then represent the statistical distribution of particles with turbulent dispersion effects. To estimate the variance of the parcel pdf due to the turbulent particle dispersion, the turbulence-induced displacement and velocity can be splitted from Eqs. (5) and (7),

$$\frac{dv_k'}{dt}=\frac{u_k'-v_k'}{\tau_k}, \tag{8}$$

$$\frac{dv_k'}{dt}=v_k'. \tag{9}$$

With the isotropic turbulence assumption, each component of u_k' is randomly chosen from a Gaussian distribution with standard deviation $u_{k_{rms}}'=\sqrt{\frac{2}{3}k}$. We first choose Δt_{ki} as the time step of the i^{th} interaction within the k^{th} eddy, which is smaller than the eddy lifetime, and integrate Eqs. (8) and (9) to update particle fluctuating locations and velocities.

$$x_{ki}'=u_{k_{rms}}'\Delta t_{ki}+(v_{k(i-1)}'-u_{k_{rms}}')\tau_{k(i-1)}\left(1-e^{\frac{-\Delta t_{ki}}{\tau_{k(i-1)}}}\right), \tag{10}$$

$$v_{ki}'=u_{k_{rms}}'+(v_{k(i-1)}'-u_{k_{rms}}')e^{\frac{-\Delta t_{ki}}{\tau_{k(i-1)}}}. \tag{11}$$

At $i=1$, we impose the initial conditions with $x_{k0}'=0$ and $v_{k0}'=0$. The mean squared dispersion at the k^{th} eddy is updated when particle begins a new interaction with a next eddy.

$$\sigma_k^2=\sigma_{k-1}^2+\left(\sum_{i=1}^{m}x_{ki}'\right)^2 \tag{12}$$

In Eq. (12), σ_{k-1} is the existing variance of the particle pdf at the begining of the interaction within the k^{th} eddy. Since the time step within

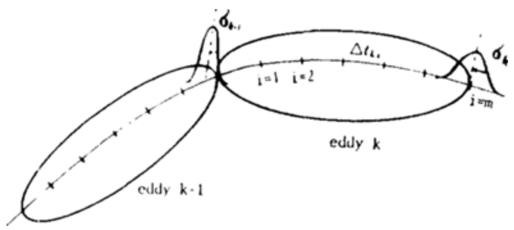

Fig. 1 Eddy interaction with the particles

each turbulent eddy is fixed, the number of interaction within the eddy, m, varies across the calculation domain, the choice of time step Δt_{k_i} and the related issues are discussed in detail in Ref.(O'Rourke, 1981). This eddy interaction with the particles is described in Fig. 1. This parcel PDF method is somewhat different from the method of Litchford and Jeng(1991) in which the calculation of the current variance of each particle pdf is summed over the entire history of the effective time constants. The present procedure is easy to program and requires less computer memory. For each computational particle, we just need to store x'_{ki}, $u'_{k_{rms}}$, v'_{ki} and σ_k^2. Furthermore, the present model includes the gas-liquid two-way coupling process and employ a two-dimensional pdf to account for the particle dispersion within a parcel (group) of particles. Two-dimensional pdf was first used by Zhou and Yao(1992) for elliptic one-way coupling flow and only one-dimensional pdf in radial direction was used by Litchford and Jeng(1991) for parabolic flows. The present study employs the one-dimensional PDF for the dilute particle dispersion with the mild axial gradients and the two-dimensional PDF for the densely loaded sprays with the large axial and radial gradients. A simplified axisymmetric cumulative distribution function in radial-direction takes the form

$$P(r)=\frac{F(r)}{F(r\to\infty)}, \tag{13}$$

where

$$\begin{aligned}F(r)=\sqrt{2\pi}\sigma_r\{&2\exp(-\frac{r_p^2}{2\sigma_r^2})\\&-\exp[-\frac{(r-r_p)^2}{2\sigma_r^2}]\\&-\exp[-\frac{(r+r_p)^2}{2\sigma_r^2}]\}\\&+\pi r_p[\mathrm{erf}(\frac{r-r_p}{\sqrt{2}\sigma_r})-\mathrm{erf}(\frac{r+r_p}{\sqrt{2}\sigma_r})\\&+2\mathrm{erf}(\frac{r_p}{\sqrt{2}\sigma_r})]\end{aligned} \tag{14}$$

and

$$\begin{aligned}F(r\to\infty)=&2\sqrt{2\pi}\sigma_r\exp(-\frac{r_p^2}{2\sigma_r^2})\\&+2\pi r_p\,\mathrm{erf}(\frac{r_p}{\sqrt{2}\sigma_r}).\end{aligned} \tag{15}$$

The error function is defined as

$$\mathrm{erf}(\eta)=\frac{2}{\sqrt{\pi}}\int_o^\eta \exp(-\zeta^2)d\zeta \tag{16}$$

and a table is used in the calculation due to no explicit analytical expression available. In axial direction, a parcel PDF is also assumed to be Gaussian with its corresponding cumulative PDF,

$$P(x)=0.5[1+\mathrm{erf}(\frac{x-x_p}{\sqrt{2}\sigma_x})]. \tag{17}$$

2.4 Turbulence modulation

The presence of the dispersed particle phase will also modulate the gas-phase turbulence structure. The effects comes into the transport equations of turbulent kinetic energy and its dissipation rate through $S_{k,p}$ and $S_{\varepsilon,p}$.

$$S_{k,p}=\overline{u_iS_{u_i,p}}-\overline{U_iS_{u_i,p}}=\overline{u'_iS_{u_i,p}} \tag{18}$$

Within the framework of discrete particle stochastic approach using Lagrangian tracking, the instantaneous properties of $S_{u_i,p}$ are known and u'_i follows the Gaussian distribution. Thus $\overline{u'_iS_{u_i,p}}$ can be calculated directly without modeling in Eq. (4). This approach is adopted in the KIVA code (Amsden et al., 1989). However, this approach requires the large number of computational particles at each control volume to minimize statistical errors. The interaction source term in ε equation is modeled as,

$$S_{\varepsilon,p}=C_3\frac{\varepsilon}{k}S_{k,p} \tag{19}$$

with $C_3=1.5$. The interphase drag force terms, $S_{u_i,p}$ are given as

$$S_{u_i,p}=-\frac{1}{dV}\sum m_pN_p\Big[\frac{U_i+u'_i-v_i}{\tau}\Big]_p$$

Here, the summation is taken only for the particles located in the grid cell, dV is the cell volume, m_p is the particle mass, N_p represents the particle number in the computational parcel. Recently, Mostafa and Mongia(1988) as well as Chen and Wood(1985) have proposed a simplified approach in which the interaction term $S_{u_{i,p}}$ is linearized followed by multiplication of the fluctuation velocity u_i'. The turbulence modulation term then only involves the gas/droplet velocity fluctuation correlation, $\overline{u_i'(u_i'-v_i')}$.

$$S_{k,p}=-\frac{1}{dV}\Sigma\frac{m_p N_p}{\tau}[\overline{u_i'(u_i'-v_i')}]_p \quad (20)$$

The interphase correlation term, $\overline{u_i'v_i'}$, is modeled through the gas-phase turbulent kinetic energy, k, the gas-phase eddy Lagrangian time scale, t_l and the particle time scale, t_d.

$$\overline{u_i'(u_i'-v_i')}=2k\, f(t_l,\ t_d) \quad (21)$$

Mostafa and Mongia's model for the above correlation is based on Chao's analysis(1962) of the linearized Lagrangian equation of motion of a spherical particle in a homogeneous turbulent flow. The function f takes the form

$$f(t_l,\ t_d)=1-\frac{t_l}{t_l+t_d}, \quad (22)$$

where t_l and t_d are given by

$$t_l=0.35\frac{k}{\varepsilon},\ t_d=\tau. \quad (23)$$

Chen et al.(1985) and Fashola et al.(1990) employed the following correction function f.

$$f(t_l,\ t_d)=1-\exp(-\frac{t_d}{t_l}), \quad (24)$$

where

$$t_l=0.5\frac{k}{\varepsilon},\ t_d=\frac{\rho_d d_p^2}{18\rho\mu}. \quad (25)$$

In these two models, the constant C_3 is taken as 1.0. In the modulation models suggested by Mostafa et al.(1988) and Chen et al.(1985), effects of different turbulent time scales with respect to particle relaxation times are incorporated in the modulation terms. Furthermore, these models simplify the evaluation procedure of the dispersed-phase source terms in two-phase flows.

2.4 Droplet breakup and collision

To account for the dense spray effects, the present study employs the Reitz's wave instability breakup model (Reitz, 1987) and an existing drop collision and coalescence model (O'Rourke, 1981). In Reitz's wave instability model, the primary and secondary breakup is modeled using a linear stability analysis for liquid jets. This breakup model (Reitz, 1987) is capable of predicting the intact core length as well as various regimes of breakup due to the action of different combinations of liquid inertia, surface tension, and aerodynamic forces on the jet. Comparative performance of the existing breakup models can be found in our previous study (Kim et al., 1994b).

The drop collision model suggested by O'Rourke(1981) is employed to calculate collision and coalescence among the dispersed liquid phase. The collision routine is operated for the pair of particles if, and only if, they are in the same computational cell. In this collision model,[9] the collision probability is assumed to follow a Poisson distribution based on a collision frequency and the computational time step. Using the probability information, the collision impact parameters are stochastically calculated. The detailed description and implementation of these dense spray models can be found in Ref.(O'Rourke, 1981; Reitz, 1987; Shang et al., 1992).

3. Solution Procedure

The gas-phase governing equations are discretized by the finite volume method. The present formulation is based on a curvilinear general coordinate with a non-staggered grid. A central differencing scheme is used for diffusion terms and a second-order upwind scheme is used for convection terms. The pressure and velocity coupling is handled by the improved PISO algorithm (Chen et al., 1992; Kim et al., 1994a). The strong coupling terms between particle and gas are evaluated by the same time splitting technique. Implicit coupling procedures are used to treat momentum exchanges to avoid the small timesteps. The discretized equations are solved by the conjugate gradient squared(CGS) method. This unsteady solution procedure for the two-phase flow calculations is different from the conventional PSIC (particle source in cell) procedure (Crowe et al., 1977) in which global iterations are required between two phases. The method used here is time-accurate and non-iterative.

For droplet/turbulence interaction calculations, integration time step is compared to the turbulent eddy life time. If the time step is smaller than the eddy time, a fluctuating component is added to the local mean gas velocity when calculating each particles mass, momentum, and energy exchange with the gas. If the time step exceeds the eddy time, turbulent changes in droplet position and velocity are chosen randomly from probability distributions for these changes as described by O'Rourke(1989). When the parcel PDF model is used, the interphase interaction source terms are redistributed according to their probability at the control volume.

4. Results and Discussions

To evaluate the present dispersion width transport model and to calibrate the stochastic simulation of particle-turbulence interactions, the computations were performed for the solid particle dispersion in a nearly-homogeneous turbulence and a particle laden round jet in inhomogeneous turbulence. The validation case for the dense spray models includes a non-evaporating solid-cone spray.

4.1 Nearly-homogeneous and inhomogeneous turbulent dispersion

The experimental setup (Snyder and Lumley, 1971) for particle dispersion in a grid-generated turbulent flow was used for evaluating the present parcel PDF model. Particle densities and sizes are chosen to examine the phenomena in which the eddy lifetime controls interaction times (46.5 μm diameter hollowgrass), the transit time controls interaction times (87.0 μm solid glass), or the controlling-interaction times undergo transition from eddy life time to transit time (87.0 μm corn pollen). In this experiment, fluid turbulence intensities and length scale information were measured. The particle calculations were started at the experimental particle injection point of $x/m = 20$ (m is a 2.54-cm-square mesh). The particle velocity was assumed equal to the mean fluid velocity of 6.55 m/sec.

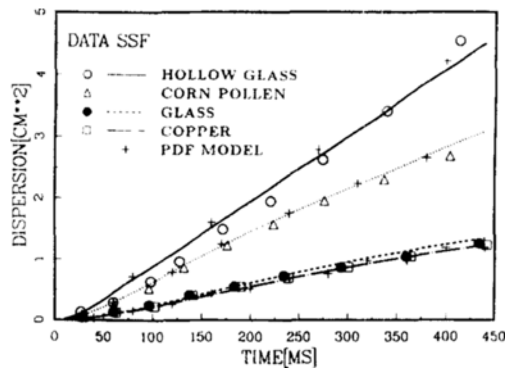

Fig. 2 Particle dispersion of a nearly-homogeneous flow for SSF model (5000 particles) and PDF model

For the delta function SSF computations, 5,000 computational particles were sampled to calculate the resulting mean squared dispersion with respect to time. For the parcel PDF computations, a single parcel in a deterministic trajectory along the centerline was sampled to evaluate the mean squared dispersion representing the variance of the parcel PDF by using the related parameters for each eddy interaction. Figure 2 shows comparison of the predicted and measured particle dispersion with respect to time. The PDF results show good agreement with the SSF results for light, medium, and heavy particles. Both models also show favourable agreement with the experimental data. These numerical results indicate that the parcel PDF model with a single computational parcel following the deterministic trajectory has the efficiency, the accuracy, and the overall prediction capability for this nearly-homogeneous turbulent flow.

The next example problem is a particle laden round jet (Yuu et al., 1978) in which the turbulence is inherently inhomogeneous. The turbulent gas-phase transport properties are provided by using the k-ε model. Figure 3 shows the particle concentration profiles of the delta function SSF model and the parcel PDF model for 200 computational parcels at several axial locations. 10,000 particles are sampled for the delta function SSF computations. Even with the 10,000 particles in the SSF model, there is still evidence of slightly insufficient sampling. However the

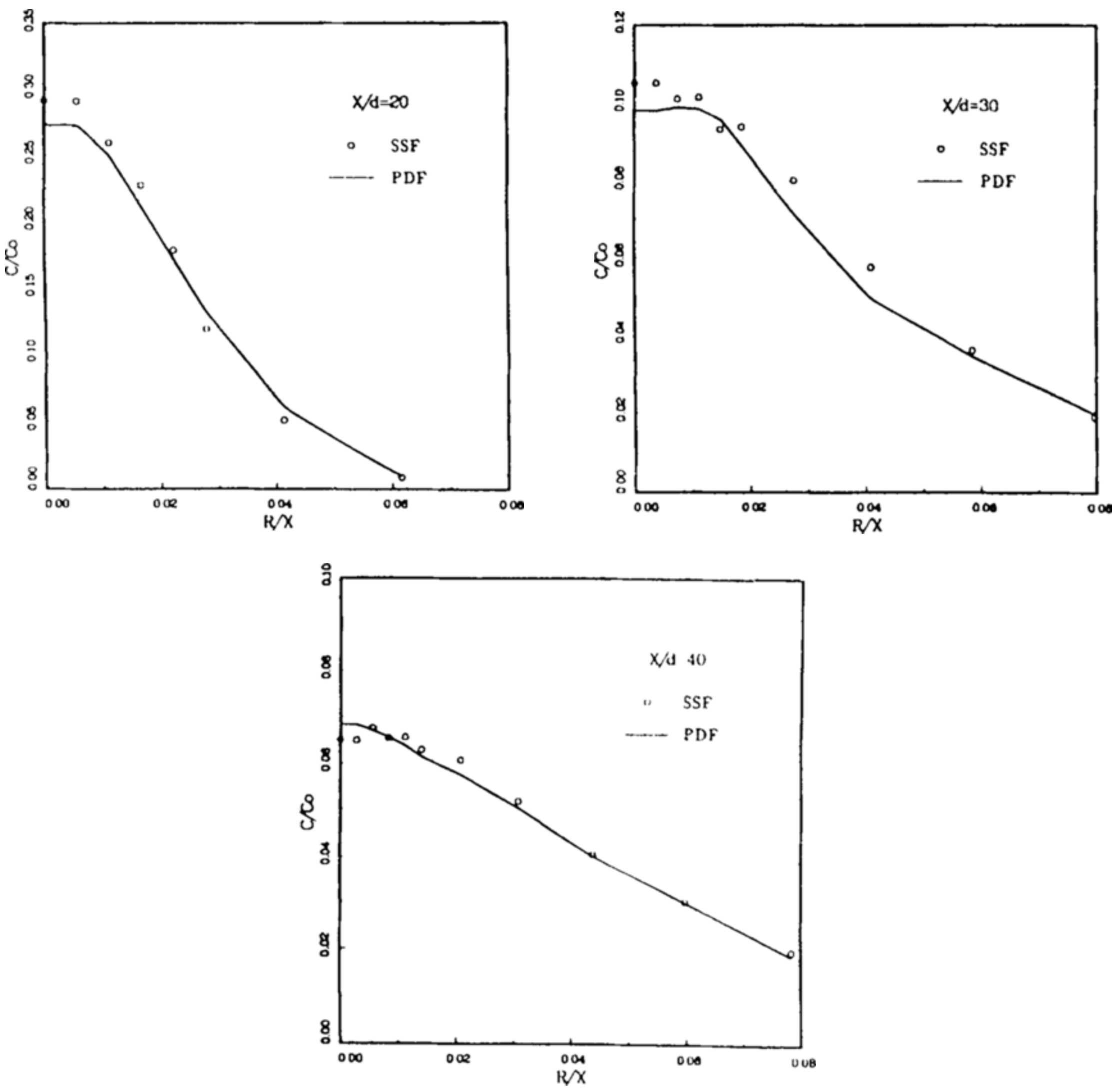

Fig. 3 Normalized particle concentration distribution of particle laden round jet for SSF model (10,000 particles) and PDF (200 parcels).

distribution is relatively smooth and is taken here as a good approximation in comparison with the parcel PDF results. In Fig. 3 the PDF results with 200 parcels show favourable agreement with the delta function SSF results with 10,000 computational particles. In terms of the CRAY X/MP CPU time, the PDF solutions with 200 parcels requires about 36 seconds while the SSF solutions with 10,000 parcels need about 1375 seconds. These numerical results clearly indicate that the parcel PDF model has the capability of accurately representing dispersion in inhomogeneous turbulent flows with improved computational efficiency over the delta function SSF model.

4.2 Non-evaporating solid-cone dense spray

The measurements of Wu et al.(1984) are selected as the validation cases to study turbulence modulations by droplets as well as to check the applicability of the present parcel PDF transport model in the dense sprays. Axial and radial components of droplet velocity were measured by laser doppler velocimeter(LDV) within liquid n-hexane sprays injecting into high-pressure nitrogen from single-hole cylindrical nozzle at room temperature. The turbulent round jet was developed by the injection of liquid fuel and its atomization. Two-phase flow was fully coupled with the gas-droplet momentum exchange especially in the immediate vicinity of the nozzle exit. Experimental conditions are described in Table 1. The dense spray effects are represented by the Reitz's wave instability breakup model (Reitz, 1987) and the collision model (O'Rourke, 1981). In the present study, the effects of drops on the turbulence are studied with the several existing modulation models. In the following figures, Model 1 corresponds to the model suggested by Mostafa et al.(1988) ; Model 2 by Amsden et al.(1989) ; Model 3 by Chen et al.(1985). Figure 4 shows the predicted gas-phase centerline velocity with and without modulation terms. Close to the nozzle, the gas-phase centerline velocity increases rapidly due to the abrupt increase of the interphase momentum transfer which results from the large relative velocities between two phases. All models predicts the peak velocity at the nearly same axial location. However, there exists differences of the centerline velocity distribution near the nozzle exit. At downstream of the peak point, the no-modulation model (standard k-ε model) predicts the fastest decay of the centerline velocity followed by Model 2, Model 1, and Model 3. In the far downstream, all models predict similar slopes due to the relatively small effects of the turbulence modulation. Therefore, the turbulence modulation is important in the jet developing region. Model 1 and Model 3 show the favorable agreement with the far-field measured velocities

Table 1 Test Conditions for the measurement of wu et al.

Case	P_{inj} (MPa)	P_{gas} (MPa)	ρ_{gas} (kg/m³)	V_{inj} (m/s)	X/d_0
A	12.5	1.48	17.02	127.0	400
B	15.2	4.24	48.68	127.0	500
C	30.4	4.24	48.68	194.0	500

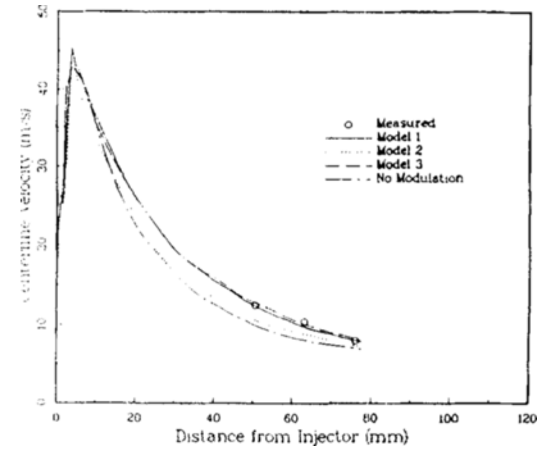

Fig. 4 Gas-phase axial centerline velocity (Case C)

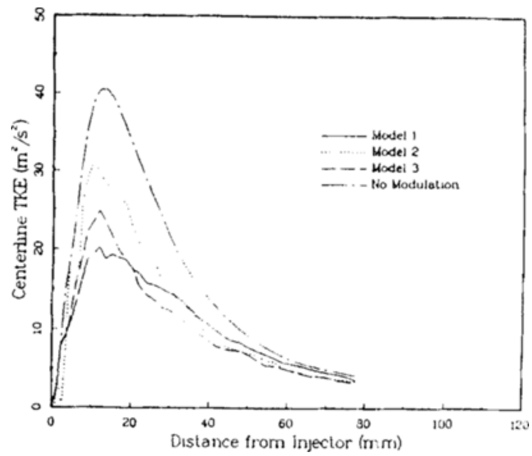

Fig. 5 Centerline turbulent kinetic energy (Case C)

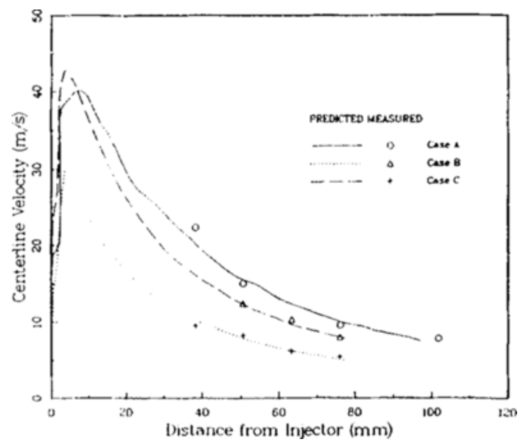

Fig. 6 Centerline velocity for three test conditions

(Case C). Figure 5 shows the centerline turbulent kinetic energy with four models. Around the peak point, Model 1 predicts the lowest turbulence level followed by Model 3, Model 2, and no-modulation model. In the far field, Model 1 and Model 3 have almost the same turbulence level. Figure 6 shows the comparison of predicted and measured centerline velocity for three test conditions of Wu et al.(1984). Predictions based on Model 1 have a good agreement with measurements for three test cases. Because of the better performance of Model 1 suggested by Mostafa et al.(1988), this model is used for the rest of validation studies.

Figure 7 shows the radial profiles of gas and drop axial mean velocity and RMS velocity at axial location of 63.5 mm (500 nozzle diameters, Case B) from the injector. The predicted mean drop velocities weighted by the drop number are obtained by averaging the instantaneous values over 6ms period. The computed mean and RMS velocities are favorably agreed with experimental data. The slight oscillations in the predicted drop velocity profile are due to insufficient sampling of computational parcels. As would be expected, the predictions for gas and drop velocities are in almost equilibrium at this downstream location. Figure 8 shows the radial profiles of the mean gas and drop velocities, and the instantaneous drop velocities using the SSF model and the parcel PDF model for case B. The number of computational parcels for the SSF model and the parcel PDF model is about 3600 in the whole flow field. Compared to the parcel PDF results, the computed profile of the SSF model is very irregular and oscillatory due to insufficient sampling. The parcel PDF model provides the realistic distributions with the mean drop profiles. Due to slightly insufficient sampling, the certain level of irregularities exists in the distributions of mean drop velocities and instantaneous droplet velocities using the parcel PDF model. Compared to the SSF calculations with the same number of computational parcels, the CPU time with the parcel PDF model is increased about 10%. However, to reach the same level of the realistic distributions as the parcel PDF model, the SSF

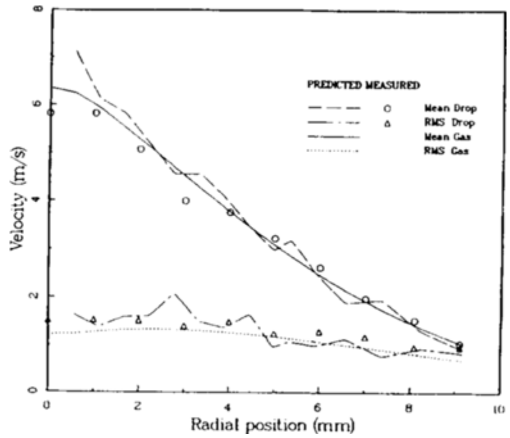

Fig. 7 Radial profiles of gas/drop axial mean and RMS velocity (Case B)

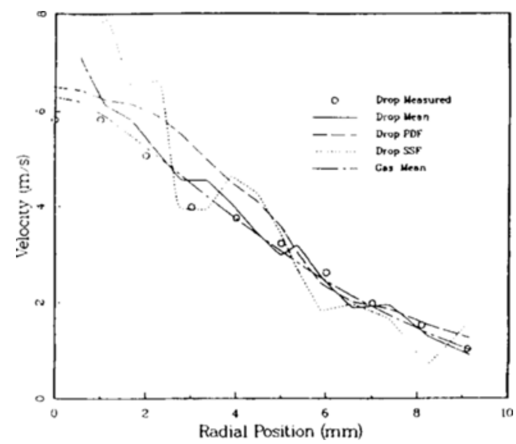

Fig. 8 Radial profiles of gas/drop mean and instantaneous axial velocity (Case B)

model needs the number of computational parcels at least several times larger which result in the drastic increase in CPU time and the memory storage requirement. Furthermore, the present parcel PDF method has potential advantages to eliminate numerically oriented noises associated with the irregular drop/gas distributions due to the insufficient sampling of computational parcels as well as to reduce the number of computational parcels with accurate representation of spray dynamics. The results indicated that the present parcel PDF model has the capability of realistically representing droplet dispersion in dense sprays with manageable number of computational parcels.

5. Conclusions

The numerical results indicate that the present parcel PDF model has the capability of realistically representing turbulent dispersion in dilute and dense sprays with improved efficiency over the delta function stochastic separated flow(SSF) model. In the non-evaporating solid-cone dense spray case, the predictions with the turbulence modulation model show a good agreement with available experimental data in terms of gas/drop mean and RMS velocities. To improve the prediction capabilities and efficiencies of the numerical and physical models, future works include the refinement of the parcel PDF model in dense sprays and the implementation of a volume-of-fluid(VOF) method to account for the effects of the volume occupied by the disperse phase in the computational cell.

References

Amsden, A. A., O'Rouke, P. J. and Butler, T. D., 1989, "KIVA-II : A Computer Program for Chemically Reactive Flows with Sprays," LA-11560-MS, Los Alamos National Lab.

Chao, B. T., 1962, "Turbulent Transport Behavior of Small Particles in Dilute Suspension," *Osterr. Ing. Arch.*, Vol. 18, pp. 7～21.

Chen, C. P. and Wood, P. E., 1985, "Turbulence Closure Model for Dilute Gas-Particle Flows," *Can. J. Chem. Engng*, Vol. 63, pp. 349～360.

Crowe, C. T., Sharma, M. P. and Stock, D. E., 1977, "The Particle Source in Cell Method for Gas-Droplet Flows," *J. Fluid Eng.*, Vol. 99, pp. 325～332.

Chen, C. P., Shang, H. M. and Jiang, Y., 1992, "A Novel Gas-Droplet Numerical Method for Spray Combustion," *Int. J. Numer. Meth. Fluids*, Vol. 15, pp. 233～245.

Chen, C. P., Jiang, Y., Kim, Y. M. and Shang, H. M., 1991, "MAST-A Multi-Phase All-Speed Transient Navier-Stokes Code in Generalized Coordinates," *NASA Contract Report*, NAG8-092, Dec.

El Banhawy, Y. and Whitelaw, J. M., 1980, "Calculation of the Flow Properties of a Confined Kerosene-Spray Flames," *AIAA J.*, Vol. 18, pp. 1503～1510.

Faeth, G. M., 1987, "Mixing, Transport and Combustion in Spray," *Prog. Energy Comb. Sci.*, Vol. 13, pp. 293～345.

Fashola, A. and Chen, C. P., 1990, "Modeling of Confined Turbulent Fluid-Particle Flows Using Eulerian and Lagrangian Schemes," *Int. J. Heat and Mass Transfer*, Vol. 33, pp. 691～700.

Kim, Y. M., Shang, H. M., Chen, C. P., Ziebarth, J. P. and Wang, T. S., 1992, "Numerical Studies of Dilute and Dense Spray Characteristics," *30th Aerospace Science Meeting*, Reno, NV. *AIAA*-92-0225.

Kim, Y. M., Shang, H. M., Chen, C. P. and Chen, Y. S., 1994a, "Prediction of Fast Transient Spray-Combusting Flows," *Numerical Heat Transfer*, Part A, Vol. 25, pp. 21～42.

Kim, Y. M., Shang, H. M., Chen, C. P. and Wang, T. S., 1994b, "Numerical Studies on Droplet Breakup Models," *J. Propulsion and Power*, Accepted for Publication.

Litchford, R. J. and Jeng, S. M., 1991, "Efficient Statistical Transport Model for Turbulent Particle Dispersion in Sprays," *AIAA J.*, Vol. 29, No. 9, pp. 1443～1451.

Mostafa, A. A. and Mongia, H. C., 1988, "On the Interaction of Particles and Turbulent Fluid Flow," *Int. J. Heat Mass Transfer*, Vol. 31, No. 10, pp. 2063～2073.

O'Rourke, P. J., 1981, "Collective Drop Effects on Vaporing Liquid Sprays," Los Alamos National Laboratory Report LA-9069-T.

O'Rourke, P. J., 1989, "Statistical Properties and Numerical Implementation of a Model for Droplet Dispersion in a Turbulent Gas," *J. Comp. Physics*, Vol. 83, pp. 345～360.

Reitz, R. D., 1987, "Modeling Atomization Processes in High-Pressure Vaporizing Sprays," *Atomization and Spray Technology*, Vol. 3, pp. 309～337.

Reitz, R.D. and Diwaker, R., 1987, "Structure of High Pressure Fuel Sprays," *SAE Paper* 870598.

Shang, H. M., Kim, Y. M., Chen, C. P. and

Wang, T. S., 1992, "Studies on Fuel Spray Characteristics in High-Pressure Environment," *28th Joint Propulsion Conf.*, *AIAA*-92-3234.

Sirignano, W. A., 1986, "The Formulation of Combustion Models: Resolution Compared to Droplet Spacing," *ASME Journal of Heat Transfer*, Vol. 108, pp. 633~639.

Shuen, J. S., Solomon, A. S., Zhang, Q. F. and Faeth, G. M., 1985, "Structure of Particle-Laden Jets: Measurements and Predictions," *AIAA J.*, Vol. 23, pp. 396~404.

Snyder, W. H. and Lumley, J. L., 1971, "Some Measurements of Particle Velocity Autocorrelation Functions in a Turbulent Flow," *J. Fluid Mech.*, Vol. 48, pp. 41~71.

Wu, K. J., Santavicca, D. A. and Bracco, F. V., 1984, "LDV Measurements of Drop Velocity in Diesel-type Sprays," *AIAA J.*, Vol. 22, p. 1263.

Yuu, S., Yasukouchi, N., Hirosawa, Y. and Jotaki, T., 1978, "Particle Turbulent Diffusion in a Dust Laden Round Jet," *AIChE Journal*, Vol. 24, No. 3, pp. 509~519.

Zhou, Q. and Yao, S. C., 1992, "Group Modeling of Impacting Spray Dynamics," *Int. J. Heat Mass Transfer*, Vol. 35, No. 1, pp.121~129.